Human Reproduction, Vol.34, No.6, pp. 978–988, 2019
Advance Access Publication on May 23, 2019 doi:10.1093/humrep/dez042

human reproduction

ORIGINAL ARTICLE *Andrology*

Sequencing of a 'mouse azoospermia' gene panel in azoospermic men: identification of *RNF212* and *STAG3* mutations as novel genetic causes of meiotic arrest

A. Riera-Escamilla[1], A. Enguita-Marruedo[2], D. Moreno-Mendoza[1], C. Chianese[3], E. Sleddens-Linkels[2], E. Contini[4], M. Benelli[5], A. Natali[6], G.M. Colpi[7], E. Ruiz-Castañé[1], M. Maggi[3], W.M. Baarends[2,*], and C. Krausz[1,3,*]

[1]Andrology Department, Fundació Puigvert, Universitat Autònoma de Barcelona, Instituto de Investigaciones Biomédicas Sant Pau (IIB-Sant Pau), 08025 Barcelona, Catalonia, Spain [2]Department of Developmental Biology, Erasmus MC University Medical Centre, 3015GD Rotterdam, The Netherlands [3]Department of Experimental and Clinical Biomedical Sciences 'Mario Serio', Centre of Excellence DeNothe, University of Florence, 50139 Florence, Italy [4]Department of Experimental and Clinical Medicine, Center of Research and Innovation of Myeloproliferative neoplasms (CRIMM), AOU Careggi, University of Florence, 50139 Florence, Italy [5]Bioinformatics Unit, Hospital of Prato, 59100 Prato, Italy [6]Department of Urology, Careggi Hospital, University of Florence, 50139 Florence, Italy [7]Department of Andrology and IVF, San Carlo Clinic, Paderno-Dugnano/Milano, 20037 Italy

*Correspondence address. Andrology Department, Fundació Puigvert, Universitat Autònoma de Barcelona, Instituto de Investigaciones Biomédicas Sant Pau (IIB-Sant Pau), 08025 Barcelona, Catalonia, Spain and Department of Experimental and Clinical Biomedical Sciences 'Mario Serio', Centre of Excellence DeNothe, University of Florence, 50139 Florence, Italy. E-mail: c.krausz@dfc.unifi.it; Department of Developmental Biology, Erasmus MC University Medical Centre, 3015GD Rotterdam, The Netherlands. E-mail: w.baarends@erasmusmc.nl

Submitted on January 7, 2019; resubmitted on February 13, 2019; editorial decision on March 5, 2019

STUDY QUESTION: What is the diagnostic potential of next generation sequencing (NGS) based on a 'mouse azoospermia' gene panel in human non-obstructive azoospermia (NOA)?

SUMMARY ANSWER: The diagnostic performance of sequencing a gene panel based on genes associated with mouse azoospermia was relatively successful in idiopathic NOA patients and allowed the discovery of two novel genes involved in NOA due to meiotic arrest.

WHAT IS KNOWN ALREADY: NOA is a largely heterogeneous clinical entity, which includes different histological pictures. In a large proportion of NOA, the aetiology remains unknown (idiopathic NOA) and yet, unknown genetic factors are likely to play be involved. The mouse is the most broadly used mammalian model for studying human disease because of its usefulness for genetic manipulation and its genetic and physiological similarities to man. Mouse azoospermia models are available in the Mouse Genome Informatics database (MGI: http://www.informatics.jax.org/).

STUDY DESIGN, SIZE, DURATION: The first step was to design of a 'mouse azoospermia' gene panel through the consultation of MGI. The second step was NGS analysis of 175 genes in a group of highly selected NOA patients ($n = 33$). The third step was characterization of the discovered gene defects in human testis tissue, through meiotic studies using surplus testicular biopsy material from the carriers of the *RNF212* and *STAG3* pathogenic variants. The final step was *RNF212* and *STAG3* expression analysis in a collection of testis biopsies.

PARTICIPANTS/MATERIALS, SETTING, METHODS: From a total of 1300 infertile patients, 33 idiopathic NOA patients were analysed in this study, including 31 unrelated men and 2 brothers from a consanguineous family. The testis histology of the 31 unrelated NOA patients was as follows: 20 Sertoli cell-only syndrome (SCOS), 11 spermatogenic arrest (6 spermatogonial arrest and 5 spermatocytic arrest). The two brothers were affected by spermatocytic arrest. DNA extracted from blood was used for NGS on Illumina NextSeq500 platform. Generated sequence data was filtered for rare and potentially pathogenic variants. Functional studies in surplus testicular tissue from the carriers

included the investigation of meiotic entry, XY body formation and metaphases by performing fluorescent immunohistochemical staining and immunocytochemistry. mRNA expression analysis through RT-qPCR of *RNF212* and *STAG3* was carried out in a collection of testis biopsies with different histology.

MAIN RESULTS AND THE ROLE OF CHANCE: Our approach was relatively successful, leading to the genetic diagnosis of one sporadic NOA patient and two NOA brothers. This relatively high diagnostic performance is likely to be related to the stringent patient selection criteria i.e. all known causes of azoospermia were excluded and to the relatively high number of patients with rare testis histology (spermatocytic arrest). All three mutation carriers presented meiotic arrest, leading to the genetic diagnosis of three out of seven cases with this specific testicular phenotype. For the first time, we report biallelic variants in *STAG3*, in one sporadic patient, and a homozygous *RNF212* variant, in the two brothers, as the genetic cause of NOA. Meiotic studies allowed the detection of the functional consequences of the mutations and provided information on the role of STAG3 and RNF212 in human male meiosis.

LIMITATIONS, REASONS FOR CAUTION: All genes, with the exception of 5 out of 175, included in the panel cause azoospermia in mice only in the homozygous or hemizygous state. Consequently, apart from the five known dominant genes, heterozygous variants (except compound heterozygosity) in the remaining genes were not taken into consideration as causes of NOA. We identified the genetic cause in approximately half of the patients with spermatocytic arrest. The low number of analysed patients can be considered as a limitation, but it is a very rare testis phenotype. Due to the low frequency of this specific phenotype among infertile men, our finding may be considered of low clinical impact. However, at an individual level, it does have relevance for prognostic purposes prior testicular sperm extraction.

WIDER IMPLICATIONS OF THE FINDINGS: Our study represents an additional step towards elucidating the genetic bases of early spermatogenic failure, since we discovered two new genes involved in human male meiotic arrest. We propose the inclusion of *RNF212* and *STAG3* in a future male infertility diagnostic gene panel. Based on the associated testis phenotype, the identification of pathogenic mutations in these genes also confers a negative predictive value for testicular sperm retrieval. Our meiotic studies provide novel insights into the role of these proteins in human male meiosis. Mutations in *STAG3* were first described as a cause of female infertility and ovarian cancer, and *Rnf212* knock out in mice leads to male and female infertility. Hence, our results stimulate further research on shared genetic factors causing infertility in both sexes and indicate that genetic counselling should involve not only male but also female relatives of NOA patients.

STUDY FUNDING/COMPETING INTEREST(S): This work was funded by the Spanish Ministry of Health Instituto Carlos III-FIS (grant number: FIS/FEDER-PI14/01250; PI17/01822) awarded to CK and AR-E, and by the European Commission, Reproductive Biology Early Research Training (REPROTRAIN, EU-FP7-PEOPLE-2011-ITN289880), awarded to CK, WB, and AE-M. The authors have no conflict of interest.

Key words: genetics / male infertility / azoospermia / spermatogenesis / gene mutations

Introduction

Male infertility is a multifactorial heterogeneous pathological condition, affecting ~7% of men. For ~40% of these cases, the aetiology remains unknown and these cases are considered as 'idiopathic'. The most severe form of male infertility is non-obstructive azoospermia (NOA), which occurs in ~1% of men of reproductive age (Tournaye *et al.*, 2016). It has been predicted that >2000 genes are involved in spermatogenesis (Mueller *et al.*, 2008) and men affected by azoospermia are at the highest risk of being carriers of genetic anomalies (Krausz and Riera-Escamilla, 2018). In fact, 15% of NOA patients carry karyotype anomalies, and Y chromosome microdeletions (azoospermia factor (AZF) deletions) are found in 8–10%. Concerning monogenic causes, massive parallel sequencing approaches have been relatively successful in identifying new candidate genetic factors, especially in patients from consanguineous families for a review, see Krausz *et al.* (2018). The majority of these studies applied the discovery-oriented approach and used the availability of the knock-out (KO) mouse reproductive phenotype for a given gene as crucial criteria for prioritization of the detected variants. The mouse is one of the most broadly used mammalian models for studying human disease because of genetic and physiological similarities between the two species (Perlman, 2016). In 2011, a study reported that more than 400 genes had so far been identified to be essential for male fertility in mice (Jamsai and O'Bryan, 2011). Alterations in these genes lead to a large range of defects during spermatogenesis (premeiotic, meiotic, or postmeiotic stages) and/or alterations at post-testicular maturation and fertilization stages (Jamsai and O'Bryan, 2011). The Mouse Genomic Informatics (MGI) website (http://www.informatics.jax.org/) provides a public database containing integrated genetic, genomic, and biological data from >60 000 mutant alleles with phenotype annotation (http://www.informatics.jax.org/). Among these >60 000 annotations, 1083 lead to disturbances in the male reproductive phenotype, from azoospermia to terato/asthenozoospermia. The aim of our study was to evaluate the frequency of mutations in genes reported in the MGI database in relationship with azoospermia, in a cohort of highly selected idiopathic NOA patients.

Materials and Methods

Subjects

From a total of 1300 infertile men attending the Fundacio Puigvert in Barcelona (Catalonia, Spain) and tested for Y chromosome microdeletions, we selected those affected by idiopathic NOA; 33 subjects gave informed consent for the present study and were enrolled. Two infertile brothers with consanguineous parents referred to the University Hospital of Careggi in Florence (Italy). These patients were

selected according to the following inclusion criteria: (i) azoospermia due to either spermatogenic arrest (at spermatogonial or spermatocytic level) or Sertoli cell-only syndrome (SCOS; type I or II); (ii) normal karyotype; (iii) absence of Y-chromosome microdeletions and *TEX11* mutations; and (iv) absence of all known causes of azoospermia. Peripheral blood samples from the patients were collected for subsequent DNA extraction and genetic analyses. The testicular phenotype of the 31 unrelated patients was as follows: 20 SCOS (17 type I and 3 type II) and 11 spermatogenic arrest (6 spermatogonial arrest and 5 speramatocytic arrest). Regarding the two brothers, both showed bilateral spermatocytic arrest. Clinical characteristics of the patients are reported in Table I. All recruited subjects signed an informed consent form and the local ethical committees of the Fundació Puigvert and of the University Hospital of Careggi approved the study.

Gene panel design

A list of genes with potential roles in azoospermia was generated by reviewing data deposited in the MGI database (http://www.informatics.jax.org/). Briefly, we searched with the keyword 'azoospermia' in the Mammalian Phenotype Browser of the MGI and selected those mutants that involve a single gene i.e. the phenotype is due to the alteration of one distinct gene. Subsequently, we searched for the human orthologs of the mouse genes by consulting the following databases: MGI and the Drosophila RNAi Screening Center (DRSC) Integrative Ortholog Prediction Tool (DIOPT; https://www.flyrnai.org/cgi-in/DRSC_orthologs.pl).

Gene panel sequencing

DNA libraries indexed with oligonucleotides compatible with Illumina's sequencing chemistry were prepared and captured using the NimbleGen SeqCap EZ Choice Library (NimbleGEn; Roche, Madison, WI) following the manufacturer's protocol. Only the coding regions and the flanking sequences (±50 nucleotides) were included for the enrichment and library preparation. The enriched libraries were quantified with Qubit (Life Technologies, Foster City, CA, USA) and Bioanalyzer 2100 (Agilent technologies, Santa Clara, California). The sequencing was performed on a NextSeq500 instrument (Illumina, San Diego, California) to generate 2 × 150 nt-long sequences with an average coverage depth of 300×. Quality of reads was checked through FastQC (http://www.bioinformatics.babraham.ac.uk/projects/fastqc/). Reads were analysed with an Illumina pipeline based on Burrows–Wheeler Aligner for sequence alignment on GRCh37 (hg19) reference, on Broad Institute Genome Analysis Toolkit (GATK) for genotyping and on Annotate Variation (ANNOVAR) for variant annotation.

Variants filtering

For the 31 unrelated azoospermic patients (sporadic cases), a standard variant filtering was applied to all samples. Briefly, we selected missense variants, stop gains/losses, and frameshift insertions/deletions, and filtered out common polymorphisms (≥5% in the general population) after consulting the dbSNP 138, the 1000G (http://www.1000genomes.org) and the genome aggregation database gnomAD (http://gnomad-old.broadinstitute.org/). The obtained data was further filtered according to their potentially damaging effect depending on the type of variant. For single nucleotide variations, the prediction of pathogenicity was based on a series of prediction tools, such as SIFT, Polyphen2_HDIV, Polyphen2_HVAR, Mutation Taster, and Mutation Assessor. An in-house index of pathogenicity (IP) was created as a score calculated on the basis of the five prediction tools employed, each providing a value ranging from 0 (null probability of being a deleterious variant) to 1 (full probability of being a deleterious variant). Not all prediction tools were always available; therefore, a ratio was calculated between the summary score of pathogenicity and the number of prediction tools available for a given variant. Hence, we established an arbitrary threshold of IP > 0.6, which means that the majority (not necessary all) of the interrogated tools gave a 'pathogenic' score (see Supplementary Table SI). We also considered as 'possibly pathogenic' all low-frequency frameshift variants and indels within non-repeated regions. Pathogenicity of the prioritized variants was also manually checked using Varsome (https://varsome.com/). Then the Integrative Genomics Viewer was employed to exclude possible false positive calls and finally, the prioritized variants were validated by Sanger sequencing.

For the two brothers from a consanguineous family, after the above-mentioned filtering, we applied the recessive model approach for further analysis. So we filtered for rare and predicted as 'pathogenic' variants that were shared by the two siblings in a hemizygous or homozygous state.

Variant validation with Sanger sequencing

To confirm the candidate variants identified in the *RNF212* and *STAG3* genes, we performed Sanger sequencing. Standard PCR was performed in a 10-µl reaction volume using the PCR Master Mix, 2× (Promega, Madison, WI, USA) and using the following protocol: 5-min initial denaturation step at 94°C, 35 cycles of 1-min denaturation at 94°C, 1-min annealing at 60°C and 1-min extension at 72°C, and a final 5-min extension at 72°C. Presence of amplification products was verified through electrophoresis on a 2% agarose gel. PCR products purification was performed by using ExoSAP-IT (Affymetrix, Santa Clara, CA, USA) in a 6-µl reaction volume, through a 15-min initial incubation at 37°C followed by a second 15-min initial incubation at 80°C. Sequencing reactions were performed using the The BigDye® Terminator v3.1 Cycle Sequencing Kit (Life Technologies) in a 10-µl reaction volume using the following protocol: 1-min initial denaturation step at 96°C and 25 cycles of 10-s denaturation at 96°C, 5-s annealing at 50°C, and 4-min extension at 60°C. Capillary electrophoresis was performed on 4-capillary 3130 Genetic Analyzer (Applied Biosystems, Carlsbad, CA, USA). We performed direct sequencing of the region of interest (ABI 3130 Genetic Analyzer). Primers are reported in Supplementary Table SII.

Quantitative RT-PCR

Quantitative RT-PCR (qRT-PCR) analysis was performed to evaluate *RNF212* and *STAG3* expression in biopsy samples of different types of adult testis histology collected in our laboratory. The extraction was performed through a combination of two commercially available kits, the TRI Reagent (Sigma-Aldrich, St. Louis, MO, USA) and the AllPrep DNA/RNA kit (Sigma-Aldrich, St. Louis, MO, USA), according to the

Table I Clinical characteristics of the selected azoospermic patients.

Patient code	Testicular histology	Sperm retrieval after TESE	FSH (IU/L)	LH (IU/L)	Testosterone (nmol/L)	Right testicular volume (cc)	Left testicular volume (cc)
13-403	SCOS type I	No	42.9	17	10.6	7	7
09-195	SCOS type II	Yes	18	n.a	n.a	10	12
08-457	SCOS type I	No	6.19	3.09	20.8	12	12
16-394	Incomplete SpermatoGonial Arrest	Yes	16.8	6.96	20.5	15	13
12-201	Incomplete SpermatoCytic Arrest	Yes	12.1	4.67	8.6	10	10
13-603	SCOS type I	No	16	12.42	11.2	12	13
11-381	SCOS type I	No	11.7	4.74	19.24	10	12
07-478	SCOS type I	No	23	9	9.4	12	12
15-546	SCOS type I	No	21.8	7.5	19.7	12	10
15-547	SCOS type I	No	13.72	7.61	15.5	10	12
15-368	SCOS type I	No	24.8	6.3	10	11	10
09-464	SCOS type I	No	20.3	n.a.	10.2	10	9
11-536	Incomplete SpermatoGonial Arrest	Yes	20	n.a.	n.a.	15	15
11-272	SpermatoCytic Arrest	No	7.16	n.a.	16	22	22
11-456	SCOS type II	No	18	9.7	14.81	12	12
14-313	SCOS type I	No	12.7	4.16	29.7	12	13
15-572	Incomplete SpermatoGonial Arrest	Yes	3.21	6.24	21.8	25	25
15-192	SCOS type I	No	19.1	10.3	25.9	11	13
07-002	SpermatoCytic Arrest	No	4.1	2.8	15.6	15	15
15-302	SCOS type I	No	22.3	5.27	24.89	12	12
15-539	SCOS type I	No	26.9	8.4	13.62	9	8
15-654	SCOS type I	No	18.1	17.22	17.2	10	10
13-400	SCOS type II	Yes	6.11	n.a.	n.a.	18	18
07-099	SCOS type I	No	6.8	2.87	n.a.	13	12
16-531	Incomplete SpermatoGonial Arrest	No	4.78	2.67	18.9	15	20
04-179	SpermatoCytic Arrest	No	20	5.9	23.9	10	12
16-639	Incomplete SpermatoGonial Arrest	No	14.66	9.85	23.4	20	18
16-702	SpermatoCytic Arrest	No	5	6.33	21.1	18	18
10-440	SCOS type I	No	25.34	18.03	10	10	4
10-499	Incomplete SpermatoGonial Arrest	Yes	4.36	2.93	20.67	20	20
16-606	SCOS type I	No	22.52	n.a.	n.a.	10	10
A1053	SpermatoCytic Arrest	No[a]	2.72	5.4	11	18	18
A1535	SpermatoCytic Arrest	No	3.62	1.77	8.3	12	12

[a]MicroTESE allowed the retrieval of few SPTs. n.a.: not available; SCOS: Sertoli cell only syndrome.

manufacturer's instructions. cDNA synthesis was carried out using the High-Capacity cDNA Reverse Transcription Kit (Life Technologies). qRT-PCR was performed using the TaqMan® Universal PCR Master Mix (Life Technologies) with the following standard thermal cycler conditions: 40 cycles at 95°C for 30 s and 60°C for 1 min. We characterized at the molecular level two samples with SCOS, two samples with spermatogonial arrest, two samples with spermatocytic arrest, and one sample with obstructive azoospermia (conserved spermatogenesis at the histological examination). This molecular characterization consisted of the expression analysis of four genes known to be expressed in different stages of spermatogenesis: *DAZ* (spermatogonia (SPG)/early spermatocytes (SPCs)), *CDY1* (spermatids (SPTs)), *BRDT* (pachytene SPCs/round and elongating SPTs), and *PRM2* (SPTs/mature spermatozoa). The housekeeping reference gene was *GAPDH*. The employed commercial assays are detailed in Supplementary Table SIII. qRT-PCR runs were performed on a StepOne™ System (Applied Biosystems). Experiments were run in triplicates.

Meiotic studies

Surplus testicular biopsy material was fixed in Bouins' fixative (brother 1) or 4% paraformaldehyde in phosphate buffered saline (PBS; brother 2 and one control (control 1) who suffered obstructive azoospermia, and displayed a Johnsen score; Johnsen, 1970) of 10 i.e. normal spermatogenesis, presence of all cell types). For the carrier of the *STAG3* mutation (07-002) and another control (control 3), the surplus testicular biopsy material was fixed in Bouins. In addition, surplus testicular biopsy material was processed to make nuclear spreads as described below for samples from brother 2 and fresh material from another control (control 2). Nuclear spreads of the sample from control 2 displayed all spermatogenic cell types. By using multiple fluorescent immunohistochemical stainings, we analysed meiotic entry, metaphase formation (including assessment of univalent presence), formation of the XY body (the silenced chromatin area in male pachytene SPCs that contains the XY chromosome pair), apoptosis, and SPT formation. Moreover, crossover (CO) frequency was determined using immunocytochemistry (using an antibody targeting the CO marker MLH1) for brother 2 and control 2. Finally, since TEX11 is thought to be stabilized by RNF212 in mice, we also measured TEX11 expression in these patients using immunohistochemistry.

Fluorescent immunohistochemistry

Testis biopsies, embedded in paraffin, were sectioned (section thickness, 6 um), and placed on a drop of demineralized H_2O on coated slides (Starfrost, Lowestoft, UK). After stretching them on a heating plate at 39°C, the water was removed and the slides were dried overnight at 37°C in an incubator. Subsequently, the slides were placed at 60°C in an oven for 1 h to melt the paraffin. Then, the slides were dewaxed and rehydrated as follows: 3 × 5 min xylene, 3 × 5 min 100% ethanol, and 3 × 5 min PBS. The slides were then incubated for 15 min in Proteinase K in PBS (1 ug/ml). This was followed by washing steps with dH_2O (4 × 2 min) and an incubation with terminal deoxynucleotidyl transferase buffer (0 0.1 M Na-cacodylate, pH 6.8, 1 0 mM CoCl, 0 1 mM DTT) for 30 min in a humid chamber. Subsequently, the slides were washed for 3 × 5 min with TB (Tris/Borate) buffer (300 mM NaCl, 30 mM tri-sodiumcitrate-dihydrate in dH2O) and 3 × 5 min with dH_2O. Thereafter, an epitope retrieval step was performed with sodium citrate buffer pH 6 (1 mM Tri-Sodium citrate (dihydrate)) in a microwave at maximum power (1 × 10 min, 2 × 5 min, and refilling the evaporated water after each microwave step). The slides were cooled down to room temperature in the sodium citrate buffer for ∼1 h, after which they were washed with PBS (3 × 5 min). Blocking was performed by incubating the sections in 10% normal goat serum and 5% bovine serum albumin (BSA) diluted in PBS, in a humid chamber for 30 min at room temperature. We used dual fluorescent staining, but with sequential incubation of the primary antibodies, as well as sequential detection, in order to reduce the risk of non-specific staining. The first primary antibody (diluted in 5% BSA/PBS) was then added to the sections and the slides were incubated in a humid chamber at 4°C overnight. The second day, the slides were first kept at room temperature for 1 h and then washed 3 × 5 min with PBS. Subsequently, the first secondary antibody (diluted in PBS) was added and the slides were incubated for 1.5 h in a humid chamber at room temperature. The slides were subsequently washed 3 × 5 minutes in PBS and incubated with the second primary antibody in 5% BSA/PBS overnight. The third day, we repeated the same steps for the detection of the second secondary antibody. Finally, slides were washed 3 × 5 minutes in PBS, and mounted using Prolong Gold Antifade reagent with DAPI.

Fluorescent immunocytochemistry

Nuclear spreads of SPCs were prepared from testis biopsies, following the protocol described by Peters *et al*. (1997). The steps of decapsulation of the tunica albuginea and placement of the cell suspension in hypobuffer solution were not performed for frozen testis biopsies (brother 2). Spread preparations of both control and patients were stored at −80°C. Thawed slides were washed in PBS (3 × 10 min), and non-specific sites were blocked with 0.5% w/v BSA and 0.5% w/v milk powder in PBS. Primary antibodies were diluted in 10% w/v BSA in PBS, and incubations were performed overnight at room temperature in a humid chamber. Subsequently, slides were washed (3 × 10 min) in PBS, blocked in 10% v/v normal goat serum (Sigma) in blocking buffer (supernatant of 5% w/v milk powder in PBS centrifuged at 14 000 rpm for 10 min), and incubated with secondary antibodies in 10% normal goat serum in blocking buffer at room temperature for 2 h. Finally, slides were washed (3 × 10 min) in PBS and embedded in Prolong Gold with DAPI (Invitrogen). Stripping of the slides was performed following the protocol described by van de Werken *et al*. (2013).

Antibodies

The following primary antibodies were used: mouse monoclonal anti-SYCP3 (Abcam:ab97672) at 1:200, rabbit polyclonal anti-SYCP3 (Lammers *et al*., 1994) at 1:750, goat polyclonal SYCP3 at 1:100 (R&D systems, Minneapolis, Minnesota), mouse monoclonal anti-MLH1 (cat. 551 091, BD Pharmigen, Franklin Lakes, New Jersey) at 1:25, mouse polyclonal anti- γH2AX at 1:750 (Millipore, Burlington, Massachusetts 05-636), mouse acrosome-specific antibody (Moore *et al*., 1987), rabbit polyclonal anti-TEX11 (Sigma: HPA002950), goat polyclonal anti-TEX11 (Abcam: 99461), human anti-centromere antibody (Crest) at 1:1000 (human centromere antiserum, Fitzgerald Industries, Tabor Ave, Manson, IA), rabbit polyclonal anti-TP2 at 1:1000 (Alfonso and Kistler, 1993), mouse monoclonal anti-protamine 1 at 1:500 (MAb-001, Briar Patch, Bessemer, Alabama), and rabbit polyclonal anti-MSH4

(Abcam: ab58666). For secondary antibodies, we used a goat anti-rabbit alexa 488 IgG, goat anti-mouse alexa 488, and goat anti-mouse alexa 546 IgG (Invitrogen), all at 1:500 dilution.

Calculation of thresholds

Based on a large cohort of patients and controls we calculated thresholds for meiotic entry, meiotic metaphase, and activation apoptosis during meiotic metaphase (manuscript to be submitted). In brief, we used the mean ± 2 SD (95% confidence interval). If the lowest/highest value of the control group was not inside this confidence interval, a Grubb's test was performed to determine if it was an outlier. In case it was not an outlier, this value was used as threshold.

Results

Gene panel

By extrapolating data from the MGI browser, we generated a gene panel that includes 175 human genes (Genes are annotated in Supplementary Table SIV). Briefly, 297 allelic compositions with different genetic backgrounds leading to azoospermia in the mouse were deposited in the Mammalian Phenotype Browser. Among them, 254 involve single-gene alterations while in 42, more than 1 gene is altered. These 254 compositions imply a total of 189 different mouse genes that cause azoospermia in mutants. For 14 of these 189 genes, no ortholog exists in human, consequently we obtained a list of 175 human genes. Among these genes, the large majority (170/175) cause azoospermia in mouse only in homozygosis. All coding exons and splicing sites of the 175 genes (168 autosomal and 7 X-linked) were sequenced as described in the Methods.

Variants identified

In the highly selected group of 31 unrelated azoospermic patients, we indentified a total of 74 low-frequency (minor allele frequency (MAF) < 0.05) and likely pathogenic variants (see Supplementary Table SV) in 49 genes in 28 patients. Of these, 72 variants belonging to 48 genes were found in heterozygosis in 27 patients and were discarded as a potential cause of azoospermia for the following reasons: (i) heterozygous mouse mutants do not show azoospermia; (ii) 13 of the 49 genes were previously reported to be associated with recessive diseases with proven paternal transmission (in OMIM), implying that the heterozygous genotype in human is not associated with azoospermia; (iii) 5 of the 49 genes cause human dominant diseases (OMIM) that were not observed in our patients, implying a lack of *in vivo* pathogenic effect of the observed variant. However, one patient (07-002) carried two variants in *STAG3* (compound heterozygosis) and was therefore subjected to further analyses.

Patient 07-002 was affected by complete bilateral meiotic arrest and carried two loss-of-function variants in *STAG3*: a frameshift insertion (NM_001282718:c.1759dupG) and a splicing variant (NM_001282716: c.2394+1G>A). The frameshift variant generates a premature stop gain in the 597th amino acid leading to a protein lacking the entire armadillo-type domain, which is predicted to be involved with DNA and protein interactions. This variant was previously reported in the gnomAD database with a MAF = 0.000004073. Concerning the splicing variant, it is a novel variant located in a canonical position (+1) in the splice donor site of exon 23 that is indispensable for normal splicing. A DNA sample from a fertile brother of patient 07-002 was available for testing by Sanger sequencing, and this analysis showed that he was a heterozygous carrier for the frameshift mutation but not for the splicing variant (Fig. 2A).

Concerning the two azoospermic brothers from the consanguineous family, we focused on shared variants and identified (i) a variant in *RNF212* (NM_001131034.3:c.111dupT) in homozygosis and (ii) three heterozygous low-frequency and likely pathogenic variants in three additional candidate genes (see Supplementary Table SV). The *RNF212* frameshift variant is located inside the zinc-finger domain and the insertion of the nucleotide leads to a premature stop gain in Lysine 38. The variant was previously described in the gnomAD database with a MAF = 0.00006582. DNA samples from the brothers' father and mother were available for testing by Sanger sequencing and analyses of their DNA showed that both parents were heterozygous carriers (Fig. 1A).

Testis expression analysis

In order to get more insight into the type of testicular cells expressing *RNF212* and STAG3, we performed a quantitative RT-qPCR analysis. This analysis shows high *RNF212* and *STAG3* mRNA expression in germ cells with the highest expression in biopsies showing spermatogonial and spermatocytic arrest. These findings suggest that, principally, early spermatogenic germ cells such as SPG and SPCs express these genes (Supplementary Fig. S1).

Meiotic studies

Analysis of meiotic entry and XY body formation

For this part of the analysis, paraffin-embedded testis biopsies were immunostained using two specific antibodies, as described in Methods. Anti-phosphorylated H2AX (gH2AX), was used to mark meiotic double-strand breaks (DSBs) and XY body formation (Mahadevaiah *et al.*, 2001). This staining served to assess progression of DSB repair as well as progression of chromosome pairing, since a clear XY body appears only when all autosomal pairs have fully synapsed. In addition, we used an antibody that detects phosphorylated H3 (H3Ser10ph), a general marker of metaphase chromosomes (Song *et al.*, 2011). According to our previously defined thresholds (manuscript to be submitted), normal meiotic entry corresponds to ≥40% early cell positive tubules (EC + T).

Patient 07-002 carrying the STAG3 mutations. In this patient with spermatocytic arrest (Fig. 2B), meiotic entry appeared to occur with normal frequency, based on the presence of many nuclei that displayed small patches of gH2AX. However, this staining was brighter compared to what we observed in the control. No XY bodies were observed. Together these results indicate persistence of meiotic DSBs and a failure to complete chromosome pairing (Fig. 2C).

Brothers carrying the RNF212 mutation. Normal meiotic entry was observed for both patients (97.8% and 86.5% EC + T, brothers 1 and 2, respectively) (Fig. 1B). Also, 100% and 98.1% of the tubules of brothers 1 and 2 displayed cells that contained XY bodies (in controls, 96.5 ± 4.5% of the counted tubules contained XY bodies), and both displayed normal XY body formation (11.2 and 10.8 for brothers 1

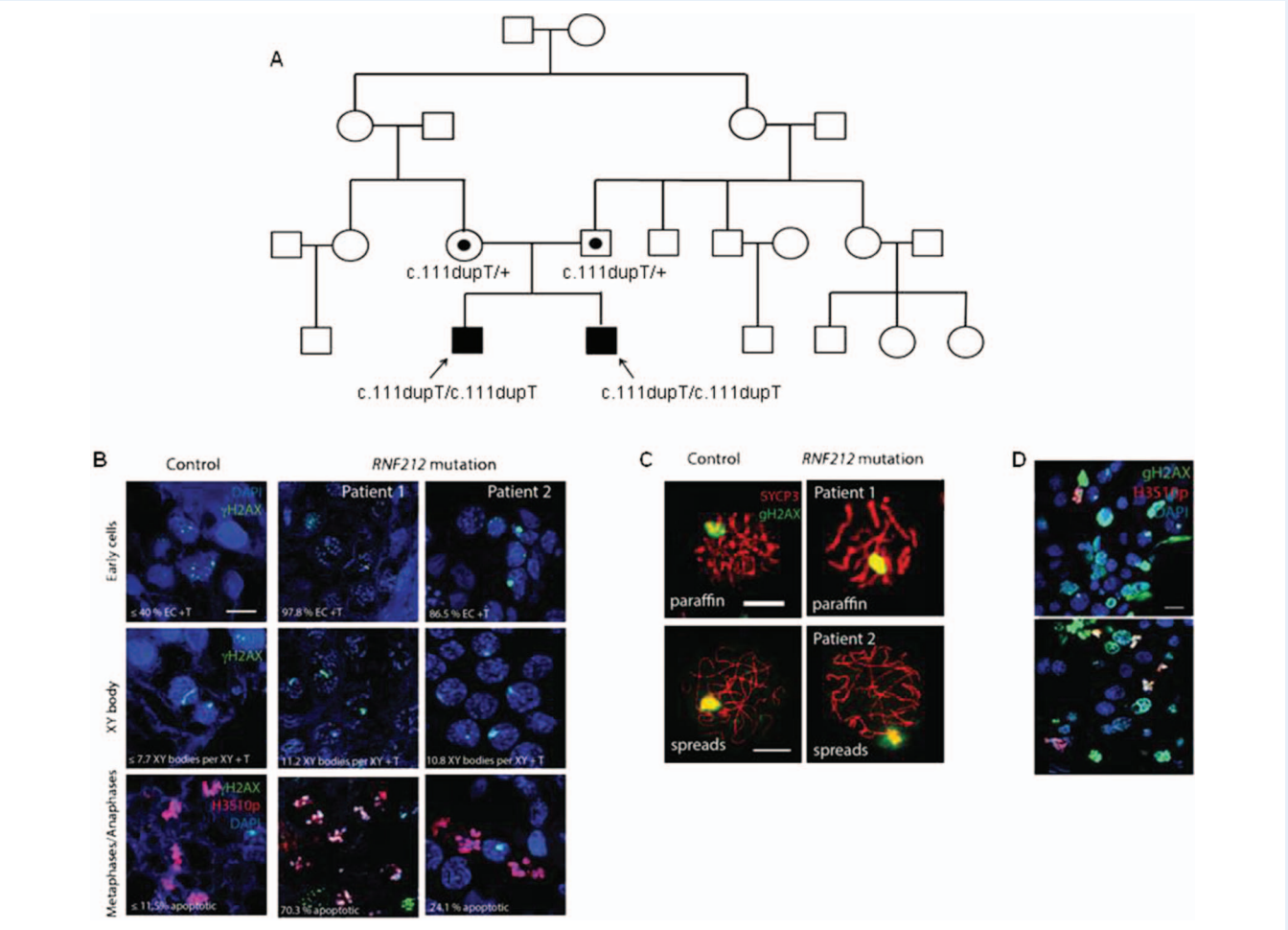

Figure 1 Investigation of the two brothers carrying the RNF212 variant. (**A**) The pedigree structure shows the segregation of the RNF212:c.111dupT variant. (**B**) Progression of meiotic prophase (early meiosis, XY body formation and metaphase/anaphase) in paraffin-embedded testis sections of control 1, brother 1, and brother 2. Immunostaining of H3Ser10ph (red) and gH2AX (red). Chromatin is stained with DAPI (blue). Thresholds for the percentage of early cell positive tubules (%EC + T), average number of XY bodies per XY body positive tubule (XY bodies per XY + T) and percentage of apoptotic metaphases, are displayed in the controls images. The values of these parameters are displayed for the patients in the correspondent images. (**C**) Pachytene nuclei of control 1 and brother 1 (paraffin-embedded testis biopsies) and control 2 and brother 2 (SPC spreads). Immunostaining of SYCP3 (red) and gH2AX (red). (**D**) Aberrant intense global gH2AX staining in tubules of brother 2. Immunostaining of H3Ser10ph (red) and gH2AX (green) on paraffin-embedded testis biopsies. Scale bar represent 10 um.

and 2, respectively; threshold ≥7.7 XY bodies per XY + T (Fig. 1B, XY body). See Methods for calculation of thresholds. Additionally, the gH2AX pattern of the pachytene SPCs was analysed in detail for both brothers (Fig. 1C). For this, anti-SYCP3 was used to mark chromosome axes in combination with anti-gH2AX on paraffin-embedded testis biopsies of brother 1 and on SPC spreads of brother 2 (more optimal for analyses of chromosome patterns). A normal gH2AX pattern and normal chromosome synapsis was observed for both patients.

Analysis of metaphases

In order to determine if the SPCs were able to complete development up to the meiotic divisions, we quantified the number of metaphases using H3S10ph as marker, and also assessed the percentage of apoptotic metaphases, using pan-chromosomal gH2AX staining in combination with a signal for H3S10ph as indicator. A threshold of 11.5% apoptotic metaphases was previously defined for the normal situation (manuscript to be submitted).

Patient 07-002 carrying the STAG3 variants. Only 2.09 metaphases/mm^2 were observed (47 metaphases/22.46-mm^2 sections). In the control sample, we counted 6.99 metaphases/mm2 (149/21.33-mm2 sections) (Fig. 2C). The average in the larger control cohort (11 obstructive azoospermia patients) that we investigated separately (manuscript submitted) was 7.54 ± 2.50, leading to a threshold of 2.53, below which we consider the number of metaphases to be below normal. In addition, we also established an upper threshold of 1.9 metaphases/mm^2 based on five patients for which we also failed to detect XY bodies in combination with absence of SPTs (manuscript submitted). Together this indicates that the SPCs were lost before they reached meiotic metaphase I.

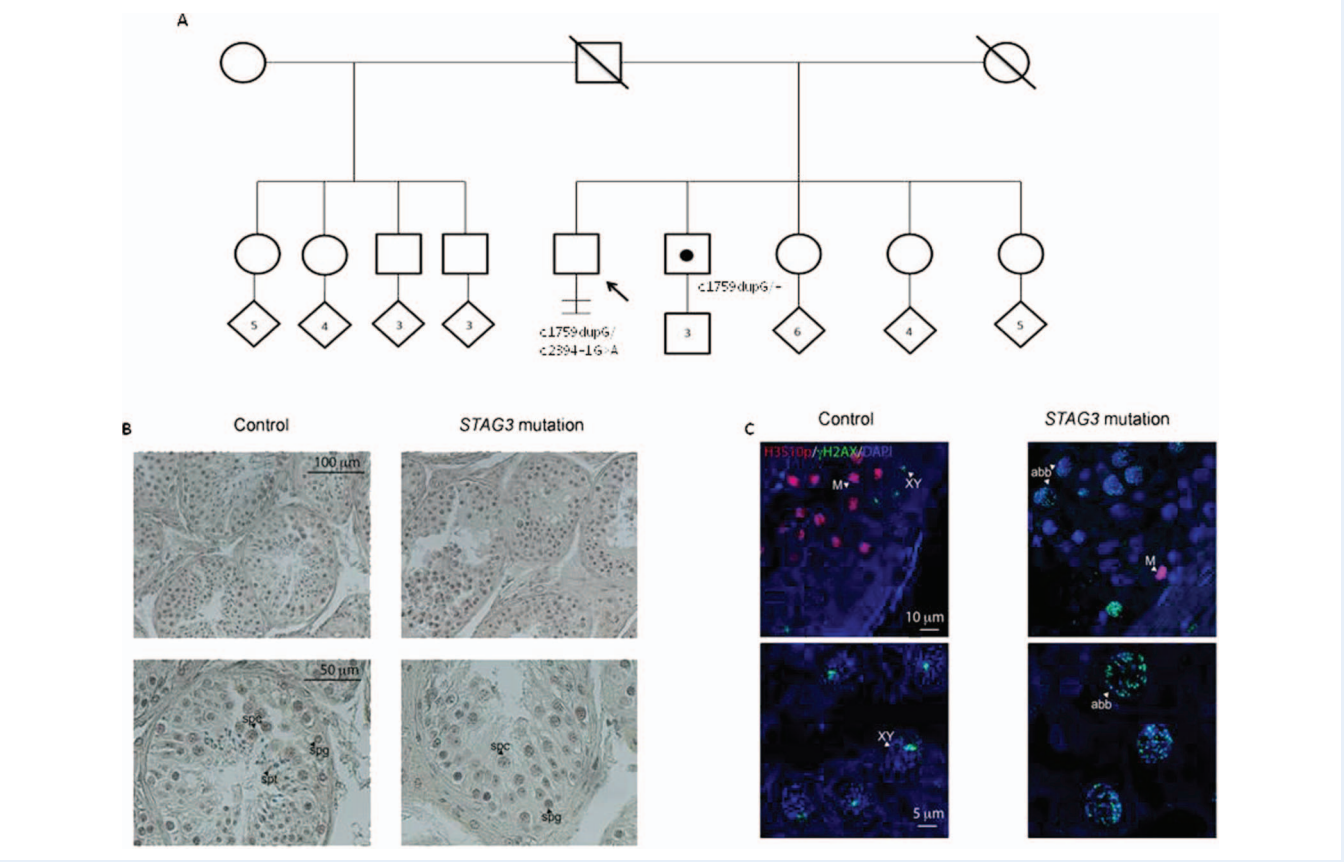

Figure 2 Investigation of the patient carrying the *STAG3* variants. (**A**) The pedigree structure shows the segregation of the STAG3 variants (c.1759dupG and c.2394 + 1G > A). The numbers inside the rhombus correspond to the number of children that each sibling has. (**B**) Histological sections (heamatoxilin-stained) of testis biopsy from control (left) and *STAG3* mutation patient (right). The control sample shows all stages of spermatogenesis, including spg, SPCs (spc), and condensed SPT. No SPTs were detected in the biopsy of the patient, but many SPCs could be observed. (**C**) Immunofluorescent detection of Histone H3 serine 10 phosphorylation (H3S10p, red, marker of M-phase), gH2AX (green, marker of DSBs and XY body), and DAPI (blue, DNA). In the control sample, a group of meiotic metaphases and anaphases is present, as well as several pachytene SPCs displaying a gH2AX-positive XY body. In the patient with the *STAG3* mutation, few metaphases were observed, and were mostly localized in the periphery, and likely representing mitoses of SPG. No XY bodies were detected, indicating that cells fail to reach pachytene. Most SPCs displayed an aberrant pattern whereby many gH2AX-positive patches covered the nuclei.

Brothers carrying the RNF212 variant. Both patients displayed a percentage of apoptotic metaphases higher than the threshold, but this percentage was much higher for brother 1 (70.3%) than for brother 2 (24.07%) (Fig. 1B, metaphases/anaphases). Only in brother 2, we also frequently observed tubules in which the majority of the nuclei (all stages) displayed aberrant intense global gH2AX staining (Fig. 1D). This suggests massive apoptosis of the nuclei inside certain tubules.

Assessment of the presence of SPTs in the brothers carrying the RNF212 variant

To assess progression of spermiogenesis in paraffin-embedded testis sections, we used an anti-acrosome antibody to detect the presence of SPTs (Florke-Gerloff *et al.*, 1983). No specific staining was obtained for the sections of brother 1. We also searched for the DAPI pattern that is characteristic of SPTs, and none were detected for this patient. For brother 2, the presence of elongated/condensed SPTs was assessed in spreads, using anti-protamine 1 antibody (Supplementary Fig. S2A). No SPTs were found. To also analyse the possible presence of early round SPTs, we used Crest (marker for the centromeres) staining, in combination with the DAPI pattern (Supplementary Fig. S2A). In the control, round SPTs displayed a characteristic DAPI-intense chromocenter, where some Crest signals are included. In contrast to previous stages (Supplementary Fig. S2A, Crest in pachytene), Crest foci displayed irregular shapes (frequently elongated) and different sizes. This type of nuclei was not found in brother 2, indicating that round SPTs were also absent. Therefore, and despite the different apoptotic responses observed for the two brothers, both were categoried as displaying complete metaphase arrest.

Reduced CO frequency and presence of univalents in brothers carrying the RNF212 variant

We analysed CO formation in both brothers, using the well-known marker MLH1. Although we obtained specific MLH1 foci in our control sample that was paraformaldehyde-fixed, only A DAPI-like non-specific staining was obtained for brother 1, indicating that anti-MLH1 did not work on Bouins'-fixed paraffin-embedded testis biopsies. For brother 2, specific SYCP3 staining but no clear MLH1 staining was obtained when using paraffin-embedded testis sections. MLH1 foci

were also absent when a SPC spreads were used for immunocytochemistry (Supplementary Fig. S2A). This suggests complete absence of crossovers.

Absence of crossovers results in the formation of univalents. To determine if they were present, a minimum of 20 metaphase/anaphase nuclei (H3Ser10ph-positive) were analysed ($n = 21$, 22, and 21 in paraffin sections from brother 1 and 2, and control 1, respectively) (Supplementary Figs S2B and S2C). Cells were categorized as metaphase when displaying only one set of chromatin or as anaphase when displaying two (Supplementary Fig. S2B). Only metaphases were observed for the control. For brother 2, most H3S10-positive cells were also at metaphase stage. In contrast, mainly anaphases were found for brother 1 (Supplementary Fig. S2C). For the patients, we sometimes observed metaphases consisting of several chromatin entities dispersed through the cell, or a few chromosomes appeared separated from the main metaphase plate (the latter was also rarely observed in the control). These entities, which probably correspond to univalents, were also observed between the two poles in anaphases in brother 1 (Supplementary Fig. S2B, anaphase of brother 1, arrowheads). In total, 2/21 (9.5%), 16/21 (76.2%), and 10/22 (45.5%) nuclei displayed clear separated chromatin entities (possible univalents) in control, brothers 1 and 2, respectively. This result shows that crossover formation is reduced in both brothers.

Analysis of TEX11 expression and localization in brothers carrying the RNF212 variant

We analysed the localization of TEX11 (together with the chromosomal axes marker SYCP3) in human SPC spread preparations (Supplementary Fig. S3A). To this end, we tested two commercially available antibodies (Sigma, St. Louis, Missouri and Abcam, Cambridge, UK), one of which (Abcam) was previously described to detect TEX11 in humans, mainly in SPTs of paraffin sections (Yatsenko *et al.*, 2015). On human spread nuclei, TEX11 foci were only observed with the Abcam antibody and appeared on synapsed axes from zygotene till pachytene in the control. This is similar to what has been described for mouse (Yang *et al.*, 2008). The same pattern was observed for brother 2 (Supplementary Fig. S3A). No apparent reduction in the number of TEX11 foci was observed in brother 2 compared to the control. For both patients and the control, we also performed DAB (3,3′-diaminobenzidine) immunohistochemistry (Supplementary Fig. S3B) for TEX11 on paraffin sections. TEX11 staining was observed in the nuclei of the SPCs, in the control and in both patients.

Discussion

The introduction of high-throughput sequencing has exponentially improved diagnostic and research yields in relation to both rare and common complex diseases. In the field of Andrology, exome analysis has been relatively successful especially for descendants of consanguineous families and familial cases of infertility (recently reviewed by Krausz *et al.*, 2018). In this study, we aimed to assess the diagnostic potential of a gene panel designed on the basis of available mouse models. We have chosen this approach because all genes included in the panel are strong candidates for spermatogenic failure in human. The availability of the mouse model for these genes made the interpretation of the obtained results straightforward. In fact, functional studies, including mouse KO, are prerequisites to attributing a disease-causing role to a newly discovered gene. Hence, we designed a gene panel that includes all monogenic models of mouse azoospermia and we sequenced the human orthologues in a cohort of 31 unrelated azoospermic patients and 2 azoospermic brothers from a consanguineous family. We identified a total of 74 low-frequency and likely pathogenic variants in 49 genes in the group of 31 unrelated NOA patients and 4 shared variants with the two brothers.

Our major finding in the cohort of 31 unrelated NOA patients is the identification of a novel gene for male infertility, *STAG3*. We describe a patient (07-002) with compound heterozygous variants in this gene. The two variants are predicted to significantly disturb the protein. The frameshift insertion causes a premature stop gain in the 597th amino acid (normal STAG3 length: 1225 amino acids) while the splicing variant located in a canonical position (+1) of the splice donor site of 23rd exon (*STAG3* has 34 exons) is predicted to affect splicing by DANN, GERP, MutationTaster, and the Human Splicing Finder (http://www.umd.be/HSF3/). *STAG3* encodes a meiosis-specific component of the cohesin complex that is necessary for (i) the correct formation of chromosome axis; (ii) the cohesion of sister chromatids after DNA replication; and (iii) DNA DSB repair during meiosis (Garcia-Cruz *et al.*, 2010; Fukuda *et al.*, 2014; Hopkins *et al.*, 2014; Llano *et al.*, 2014; Winters *et al.*, 2014; Ward *et al.*, 2016; Nambiar and Smith, 2018). Various mutations (frameshift, splicing, and missense) have been already reported in *STAG3* as a cause of premature ovarian insufficiency (POI) (Caburet *et al.*, 2014; Le Quesne Stabej *et al.*, 2016; Colombo *et al.*, 2017; Franca *et al.*, 2018; He *et al.*, 2018). In four out of five familial POI cases, the mutations were in homozygosis since the carriers were from consanguineous families (Caburet *et al.*, 2014; Le Quesne Stabej *et al.*, 2016; Colombo *et al.*, 2017; He *et al.*, 2018). The first woman with POI-carrying compound heterozygous variants in this gene was reported recently by Franca *et al.* (2018). *STAG3* is a strong candidate for male infertility because male mice lacking *Stag3* display a severe meiotic arrest phenotype (Llano *et al.*, 2014) and in the MGI database, mice (both male and female) are reported to be infertile due to azoospermia and absence of oocytes, respectively. Our observation of lack of XY body formation, persistent gH2AX foci, and failure to reach meiotic metaphase are consistent with the STAG3-deficient mouse phenotype. The use of remnant testis biopsy material for the immunofluorescent assessment of meiotic progression provides patient-relevant information since it allowed us to determine that in man, similar to mouse, STAG3 is required for proper meiotic chromosome pairing. Hence, it should be considered that if rare SPTs that may form in the testis of this patient would be found, they would most likely be genetically abnormal, and the patient should be informed of this likely risk.

Thus, for the first time in the literature, we report causative mutations in *STAG3* in human azoospermia that is clearly associated with a negative predictive value for testicular sperm retrieval.

Concerning the familial case, we identified a homozygous pathogenic variant in *RNF212* (NM_001131034.3:c.111dupT) shared by the two brothers. The truncating mutation is located inside the zinc-finger domain and creates a new stop gain in the 38th amino acid (total RNF212 protein length is 297 amino acids). The protein encoded by *RNF212* is a RING-family E3-ligase required for chiasm formation and assembly of crossover-specific recombination complexes (Reynolds *et al.*, 2013; Qiao *et al.*, 2014, 2018; Rao *et al.*, 2017). Studies on mouse

models show that the RNF212 protein functions to couple chromosome synapsis to the formation of crossover-specific recombination complexes (Reynolds *et al.*, 2013). *Rnf212* mutation in mice causes sterility in both sexes and, in particular, *Rnf212* KO mice are sterile due to the loss of SPCs at post-anaphase stage (Reynolds *et al.*, 2013). Consistently, when testicular sperm extraction (TESE) was attempted for the two brothers, 90% of the tubules suffered spermatogenic arrest at the SPC level. In addition, our immunofluorescent analyses of both brothers showed that SPCs reached pachytene, but underwent apoptosis during the first meiotic division (metaphase or anaphase). In addition, univalents were frequently observed. In *Rnf212*$^{-/-}$ mice, crossing over is diminished by ≥90%, as expected (Reynolds *et al.*, 2013). We observed that 76.2% and 45.5% metaphase/anaphase cells contain possible univalents for brothers 1 and 2, respectively. Although we could not detect MLH1 foci, the appropriate metaphase alignment of at least some bivalents, suggests that some crossovers still form in our *RNF212* patients. A reduction in the number of crossovers and metaphase arrest has also been observed in male mice upon deletion of the X-linked *Tex11* (Yang *et al.*, 2008). TEX11 is thought to be stabilized by RNF212, and the number of TEX11 foci is markedly lower (around 6 times less foci) upon deletion of *Rnf212* in male mice (Reynolds *et al.*, 2013). Nevertheless, our analysis suggests that TEX11 foci formation is not affected by the *RNF212* mutation in our patients. So, although we have shown here that the meiotic localization and expression pattern of TEX11 is similar in mouse and man, in contrast to what was previously observed (Yatsenko *et al.*, 2015), our data suggests that the functional interaction between RNF212 and TEX11 may be somewhat different in man compared to that in mouse.

In conclusion, by using a hypothesis-driven approach, which consisted of the sequencing of the 175 genes, we obtained a genetic diagnosis in one sporadic NOA patient and in two NOA brothers. Ours is the first study reporting biallelic variants in *STAG3* in one sporadic patient and a homozygous *RNF212* variant in the two brothers as the genetic cause of NOA. All three mutation carriers presented meiotic arrest leading to the genetic diagnosis of three of seven cases with this specific testicular phenotype. Our study represents an additional step towards elucidating the genetic basis of early spermatogenic failure, since we report two new genes involved in human male meiotic arrest. We propose the inclusion of *RNF212* and *STAG3* in a future male infertility-diagnostic gene panel. Meiotic studies also allowed the detection of the functional consequences of the mutations and provided information on the role of STAG3 and RNF212 in human male meiosis.

More than half of the 175 sequenced genes are also reported to affect also female reproduction in mice (among them *Rnf212 and Stag3*) and *STAG3* mutations were first described as a cause of female infertility (POI) and ovarian cancer. Hence, our results stimulate further research on shared genetic factors causing both POI and NOA. The diagnosis of such genetic factors implies that genetic counselling for NOA has relevance not only to the male family members and male descendants but also to female relatives.

Supplementary data

Supplementary data are available at *Human Reproduction* online.

Acknowledgements

The authors wish to thank the patients participating in the study for their important collaboration. We also thank the clinicians from the Andrology Unit of the Fundació Puigvert (J.Sarquella, J. Sanchez-Curbelo) who helped provide samples for this study and Sara Pietroforte (University of Florence) for her help in the bioinformatics analyses. A special acknowledgment is dedicated to Esperança Martí, President of the Fundació Puigvert, for her constant support. In addition we wish to thank Vera de Geus and Lieke Koornneef (Erasmus MC Medical Center Rotterdam, The Netherlands) for their assistance in the immunostainings.

Authors' roles

ARE: bioinformatic investigation, sample preparation, resequencing, qPCR experiments, data analysis, interpretation of results, and manuscript preparation; AEM: analysis and interpretation of the meiotic studies and manuscript preparation; DMM, AN, GMC, ERC, MM: recruitment of patients and acquisition of clinical data; CC: sample preparation, resequencing, data analysis; ESL: meiotic studies; EC and MB: bioinformatic analysis; WMB: supervision and interpretation of the meiotic studies, manuscript preparation; CK: study conception and design, study supervision, data interpretation, and manuscript preparation.

Funding

Spanish Ministry of Health Instituto Carlos III-FIS (grant number FIS/FEDER-PI14/01250; PI17/01822), the European Commission, Reproductive Biology Early Research Training (REPROTRAIN, project number: 289880, awarded to CK and AR-E), and European Commission through EU-FP7-PEOPLE-2011-ITN289880 (awarded to WB and AE-M).

Conflict of interest

The authors declare no conflict of interest.

References

Alfonso PJ, Kistler WS. Immunohistochemical localization of spermatid nuclear transition protein 2 in the testes of rats and mice. *Biol Reprod* 1993;**48**:522–529.

Caburet S, Arboleda VA, Llano E, Overbeek PA, Barbero JL, Oka K, Harrison W, Vaiman D, Ben-Neriah Z, Garcia-Tunon I *et al.* Mutant cohesin in premature ovarian failure. *N Engl J Med* 2014;**370**:943–949. United States.

Colombo R, Pontoglio A, Bini M. A STAG3 missense mutation in two sisters with primary ovarian insufficiency. *Eur J Obstet Gynecol Reprod Biol* 2017;**216**:269–271. Ireland.

Florke-Gerloff S, Topfer-Petersen E, Muller-Esterl W, Schill WB, Engel W. Acrosin and the acrosome in human spermatogenesis. *Hum Genet* 1983;**65**:61–67. Germany.

Franca MM, Nishi MY, Funari MFA, Lerario AM, Baracat EC, Hayashida SAY, Maciel GAR, Jorge AAL, Mendonca BB. Two rare

loss-of-function variants in the STAG3 gene leading to primary ovarian insufficiency. *Eur J Med Genet* 2018;Mar;**62**(3):186–189. Netherlands.

Fukuda T, Fukuda N, Agostinho A, Hernandez-Hernandez A, Kouznetsova A, Hoog C. STAG3-mediated stabilization of REC8 cohesin complexes promotes chromosome synapsis during meiosis. *EMBO J* 2014;**33**:1243–1255. England.

Garcia-Cruz R, Brieno MA, Roig I, Grossmann M, Velilla E, Pujol A, Cabero L, Pessarrodona A, Barbero JL, Garcia Caldes M. Dynamics of cohesin proteins REC8, STAG3, SMC1 beta and SMC3 are consistent with a role in sister chromatid cohesion during meiosis in human oocytes. *Hum Reprod* 2010;**25**:2316–2327. England.

He W-B, Banerjee S, Meng L-L, Du J, Gong F, Huang H, Zhang X-X, Wang Y-Y, Lu G-X, Lin G *et al.* Whole-exome sequencing identifies a homozygous donor splice-site mutation in STAG3 that causes primary ovarian insufficiency. *Clin Genet* 2018;**93**:340–344. Denmark.

Hopkins J, Hwang G, Jacob J, Sapp N, Bedigian R, Oka K, Overbeek P, Murray S, Jordan PW. Meiosis-specific cohesin component, Stag3 is essential for maintaining centromere chromatid cohesion, and required for DNA repair and synapsis between homologous chromosomes. *PLoS Genet* 2014;**10**:e1004413. United States.

Jamsai D, O'Bryan MK. Mouse models in male fertility research. *Asian J Androl* 2011;**13**:139–151. China.

Johnsen SG. Testicular biopsy score count–a method for registration of spermatogenesis in human testes: normal values and results in 335 hypogonadal males. *Hormones* 1970;**1**:2–25.

Krausz C, Cioppi F, Riera-Escamilla A. Testing for genetic contributions to infertility: potential clinical impact. *Expert Rev Mol Diagn* 2018;**18**: 331–346. England.

Krausz C, Riera-Escamilla A. Genetics of male infertility. *Nat Rev Urol* 2018;**15**:369–384. England.

Lammers JH, Offenberg HH, van AM, Vink AC, Dietrich AJ, Heyting C. The gene encoding a major component of the lateral elements of synaptonemal complexes of the rat is related to X-linked lymphocyte-regulated genes. *Mol Cell Biol* 1994;**14**:1137–1146. United States.

Le Quesne Stabej P, Williams HJ, James C, Tekman M, Stanescu HC, Kleta R, Ocaka L, Lescai F, Storr HL, Bitner-Glindzicz M *et al.* STAG3 truncating variant as the cause of primary ovarian insufficiency. *Eur J Hum Genet* 2016;**24**:135–138. England.

Llano E, Gomez-H L, Garcia-Tunon I, Sanchez-Martin M, Caburet S, Barbero JL, Schimenti JC, Veitia RA, Pendas AM. STAG3 is a strong candidate gene for male infertility. *Hum Mol Genet* 2014;**23**:3421–3431. England.

Mahadevaiah SK, Turner JM, Baudat F, Rogakou EP, de BP, Blanco-Rodriguez J, Jasin M, Keeney S, Bonner WM, Burgoyne PS. Recombinational DNA double-strand breaks in mice precede synapsis. *Nat Genet* 2001;**27**:271–276. United States.

Moore HDM, Smith CA, Hartman TD, Bye AP. Visualization and characterization of the acrosome reaction of human spermatozoa by immunolocalization with monoclonal antibody. *Gamete Res* 1987;**17**:245–259.

Mueller JL, Mahadevaiah SK, Park PJ, Warburton PE, Page DC, Turner JMA. The mouse X chromosome is enriched for multicopy testis genes showing postmeiotic expression. *Nat Genet* 2008;**40**:794–799. United States.

Nambiar M, Smith GR. Pericentromere-specific cohesin complex prevents meiotic pericentric DNA double-strand breaks and lethal crossovers. *Mol Cell* 2018;**71**:540–553.e4. United States.

Perlman RL. Mouse models of human disease: An evolutionary perspective. *Evol Med public Heal* 2016;**2016**:170–176. England.

Peters AH, Plug AW, van VMJ, de BP. A drying-down technique for the spreading of mammalian meiocytes from the male and female germline. *Chromosome Res* 1997;**5**:66–68. Netherlands.

Qiao H, Prasada Rao HBD, Yang Y, Fong JH, Cloutier JM, Deacon DC, Nagel KE, Swartz RK, Strong E, Holloway JK *et al.* Antagonistic roles of ubiquitin ligase HEI10 and SUMO ligase RNF212 regulate meiotic recombination. *Nat Genet* 2014;**46**:194–199. United States.

Qiao H, Rao HBDP, Yun Y, Sandhu S, Fong JH, Sapre M, Nguyen M, Tham A, Van BW, Chng TYH *et al.* Impeding DNA break repair enables oocyte quality control. *Mol Cell* 2018;**72**:211–221.e3. United States.

Rao HBDP, Qiao H, Bhatt SK, Bailey LRJ, Tran HD, Bourne SL, Qiu W, Deshpande A, Sharma AN, Beebout CJ *et al.* A SUMO-ubiquitin relay recruits proteasomes to chromosome axes to regulate meiotic recombination. *Science* 2017;**355**:403–407. United States.

Reynolds A, Qiao H, Yang Y, Chen JK, Jackson N, Biswas K, Holloway JK, Baudat F, de Massy B, Wang J *et al.* RNF212 is a dosage-sensitive regulator of crossing-over during mammalian meiosis. *Nat Genet* 2013;**45**: 269–278. NIH Public Access.

Song N, Liu J, An S, Nishino T, Hishikawa Y, Koji T. Immunohistochemical analysis of histone H3 modifications in germ cells during mouse spermatogenesis. *Acta Histochem Cytochem* 2011;**44**:183–190. Japan.

Tournaye H, Krausz C, Oates RD. Novel concepts in the aetiology of male reproductive impairment. *Lancet Diabetes Endocrinol* 2016;Jul;**5**(7):544–553. England.

van de Werken C, Jahr H, Avo Santos M, Eleveld C, Schuilwerve J, Laven JSE, Baart EB. A universal method for sequential immunofluorescent analysis of chromatin and chromatin-associated proteins on chromosome spreads. *Chromosome Res* 2013; **21**:475–489.

Ward A, Hopkins J, Mckay M, Murray S, Jordan PW. Genetic interactions between the meiosis-specific cohesin components, STAG3, REC8, and RAD21L. *G3 (Bethesda)* 2016;**6**:1713–1724. United States.

Winters T, McNicoll F, Jessberger R. Meiotic cohesin STAG3 is required for chromosome axis formation and sister chromatid cohesion. *EMBO J* 2014;**33**:1256–1270. England.

Yang F, Gell K, van der Heijden GW, Eckardt S, Leu NA, Page DC, Benavente R, Her C, Höög C, McLaughlin KJ *et al.* Meiotic failure in male mice lacking an X-linked factor. *Genes Dev* 2008; **22**:682–691.

Yatsenko AN, Georgiadis AP, Ropke A, Berman AJ, Jaffe T, Olszewska M, Westernstroer B, Sanfilippo J, Kurpisz M, Rajkovic A *et al.* X-linked TEX11 mutations, meiotic arrest, and azoospermia in infertile men. *N Engl J Med* 2015;**372**:2097–2107. United States.